the ligand in the two binding sites when the protein coordinates become available.

ACKNOWLEDGMENTS

NMR processing, display, and plotting routines were written by Dennis Hare, and integration routines were written by J. N. Scarsdale and Paul-James Jones.

REFERENCES

Araki, T., & Funatsu, G. (1985) *FEBS Lett. 191*, 121.
Clore, G. M., & Gronenborn, A. M. (1982) *J. Magn. Reson. 48*, 402.
Fischer, E., & Fischer, H. (1910) *Ber. Dtsch. Chem. Ges. 43*, 2521.
Hatakeyama, T., Yamasaki, N., & Funatsu, G. (1986) *J. Biochem. 99*, 1049.
Hirotsu, K., & Shimada, A. (1974) *Bull. Chem. Soc. Jpn. 47*, 1872.
Houston, L. L., & Dooley, T. P. (1982) *J. Biol. Chem. 257*, 4147.
Jeener, J., Meier, B. H., Bachmann, P., & Ernst, R. R. (1979) *J. Chem. Phys. 71*, 4546.
Koch, H. J., & Stuart, R. S. (1978) *Carbohydr. Res. 67*, 341.
Kumar, A., Ernst, R. R., & Wüthrich, K. (1980) *Biochem. Biophys. Res. Commun. 95*, 1.
Montfort, W., Villafranca, J. E., Monzingo, A. F., Ernest, S. R., Katzin, B., Rutenber, E., Xuong, N. H., Hamlin, R., & Robertus, J. D. (1987) *J. Biol. Chem. 262*, 5398.
Olsnes, S., & Pihl, A. (1982) in *Molecular Aspects of Cellular Regulation* (Cohen, P., & Van Heyningen, S., Eds.) Vol. 2, pp 51–105, Elsevier Biomedical Press, Amsterdam.
Olsnes, S., Refsnes, K., Christensen, T. B., & Pihl, A. (1975) *Biochim. Biophys. Acta 405*, 1.
Paulsen, H., Hasenkamp, T., & Paal, M. (1985) *Carbohydr. Res. 144*, 45.
Rutenber, E., Ready, M., & Robertus, J. D. (1987) *Nature 326*, 624.
Scarsdale, J. N. (1989) Ph.D. Thesis, Yale University, New Haven, CT.
Scarsdale, J. N., Ram, P., & Prestegard, J. H. (1988) *J. Comput. Chem. 9*, 133.
Smith, F., & Van Cleve, J. W. (1952) *J. Am. Chem. Soc. 74*, 1912.
States, D. J., Haberkorn, R. A., & Ruben, D. J. (1982) *J. Magn. Reson. 48*, 286.
Sundler, R., & Wijkander, J. (1983) *Biochim. Biophys. Acta 730*, 391.
Takagi, S., & Jeffrey, G. A. (1978) *Acta Crystallogr. B34*, 2006.
Wider, G., Macura, S., Kumar, A., Ernst, R. R., & Wüthrich, K. (1984) *J. Magn. Reson. 56*, 207.
Yamasaki, N., Hatakeyama, T., & Funatsu, G. (1985) *J. Biochem. 98*, 1555.

O_2 and CO Reactions with Heme Proteins: Quantum Yields and Geminate Recombination on Picosecond Time Scales†

Mark R. Chance,*,‡ Scott H. Courtney,§ Mark D. Chavez,∥ Mark R. Ondrias,∥ and Joel M. Friedman§

Department of Chemistry, Georgetown University, 37th and O Street, N.W., Washington, D.C. 20057, AT&T Bell Laboratories, Murray Hill, New Jersey 07974, and Department of Chemistry, University of New Mexico, Albuquerque, New Mexico 87131

Received December 14, 1989; Revised Manuscript Received February 6, 1990

ABSTRACT: Picosecond time-resolved absorption spectroscopy and low-temperature studies have been undertaken in order to understand the nature of the intrinsic quantum yields and geminate recombination of carbon monoxide and oxygen to hemoglobin and myoglobin. We find that the photoproduct yields at 40 ps and long times (minutes) after photolysis at 8 K are similar; however, the yield of oxygen photoproducts is 0.4 ± 0.1 while the yield of carbon monoxide photoproducts is 1.0 ± 0.1 for both myoglobin and hemoglobin. Measurements in the Soret, near-infrared, and far-IR are used to quantitate the photoproduct yields. These results call into question previous cryogenic kinetic studies of O_2 recombination. Significant subnanosecond geminate recombination is observed in oxyhemoglobin down to 150 K, while below 100 K this geminate recombination disappears. The lower photoproduct yields for oxyheme protein complexes can be attributed to both subnanosecond and subpicosecond recombination events which are ligand and protein dynamics dependent.

Characterization of the photolytic reactions of ligand-bound hemoglobin and myoglobin is essential for understanding the kinetics and reactivity of heme reactions (Gibson, 1959; Antonini & Brunori, 1971; Gibson & Antonini, 1967). In general, the photoproduct yields are quite ligand-specific with the observed yield of photolysis products for NO and O_2 invariably lower than those for CO ligand. For example, the photoproduct yield for horse CO myoglobin on microsecond time scales is 1.0, while those for O_2 and NO ligands are 0.03 and 0.001, respectively (Antonini & Brunori, 1971). In addition, observed yields are affected by temperature, solution conditions, and protein structure (Gibson & Ainsworth, 1959; Saffran & Gibson, 1977; Brunori et al., 1973; Noble et al., 1967).

A major advance in the study of ligand–heme protein photodissociative events occurred with the discovery that geminate recombination on the 100-ns time scale contributes to the observed differences in longer time photoproduct yields (Duddell et al., 1979; Alpert et al., 1979; Friedman & Lyons,

† This work was supported in part by National Science Foundation Grant DMB-8604435.

* Address correspondence to this author.
‡ Georgetown University.
§ AT&T Bell Laboratories.
∥ University of New Mexico.

0006-2960/90/0429-5537$02.50/0

1980). In fact, the differences in the yield of CO photolysis on microsecond and longer time scales between hemoglobin and myoglobin originate almost entirely from differences in geminate recombination processes (Friedman & Lyons, 1980; Hofrichter et al., 1985). Subsequently, picosecond (Chernoff et al., 1980; Cornelius et al., 1983; Friedman et al., 1985) and femtosecond (Martin et al., 1983; Jongeward et al., 1987) studies have demonstrated ligand-specific geminate phases occurring over a wide range of time scales.

The room temperature solution-phase studies have clearly exposed the role of both intraprotein dynamics and the energetics of heme–ligand recombination processes contributing to the overall observed photolysis yield at longer times. In addition, they provide a link between photoproduct yields under ambient conditions and the cryogenic studies of Frauenfelder and co-workers that also deal with protein dynamics and the various barriers to ligand recombination within the protein at low temperatures (Austin et al., 1975; Alberding et al., 1978; Doster et al., 1982; Ansari et al., 1985, 1986). These cryogenic studies reveal several cryogenic processes in series that contribute to the overall ligand recombination dynamics. Below 180 K, only a single intraprotein recombination process is operative. This geminate phase, termed "process I", is characterized by a distribution of recombination rates controlled by a distribution of potential energy barrier heights. The structural basis of the barrier distribution is asserted to be a distribution of conformational substates that are similar in overall structure but differ in their microscopic details and in their rebinding rates. Recent kinetic hole-burning experiments (Campbell et al., 1987; Agmon, 1988) provide spectroscopic support for this picture that conformational substates are responsible for the distribution in rebinding rates in photodissociated MbCO.

A significant focus of both ambient and cryogenic studies is to discern the molecular basis for the large differences in reactivity between CO and O_2 in their interactions with Hb and Mb. For ambient solution-phase experiments, the ligand-specific differences are manifest in the reduced photolytic yield and enhanced geminate yield for O_2 over CO.

Martin et al. (1983) have shown that the disappearance of liganded states occurs immediately upon photolysis (<50 fs), while deoxy-like Soret species are observed later, after 300 fs. Recently, femtosecond transient absorption investigations by Petrich et al. (1988) have provided evidence for ultrafast (subpicosecond) recombination of O_2 and NO ligands with hemoglobin and myoglobin. They attribute these ultrafast processes to decay of an electronically excited geminate pair. This model suggests that observed yields are influenced by electronic processes at early times (<5 ps).

In this context, the early time photolytic yield would originate from ligand-dependent branching ratios for (at least) two relaxation pathways, one leading to a deoxy-like photoproduct and the other to the initial ligand-bound species. Alternatively, it has been suggested (Agmon & Hopfield, 1983) that the distribution of barrier heights controlling geminate rebinding at either cryogenic or ambient temperatures can include contributions from conformational substates having a near-zero or zero barrier height. Such conformational substates would presumably recombine on ultrafast time scales. A relevant question is to what extent is the distribution of barrier heights different for O_2 and CO? Is the O_2 distribution *tilted in* favor of states that have little or no barrier to rebinding?

The literature concerning the low-temperature kinetics of O_2 and CO recombination with hemoglobin and myoglobin is extensive and has included the monitoring of recombination in the Soret, near-infrared, and far-infrared regions of the spectrum (Austin et al., 1975; Doster et al., 1982; Ansari et al., 1985, 1986, 1987; Chance et al., 1987). On the basis of such studies, it was concluded that MbO_2 and MbCO have a very similar distribution of enthalpic barrier heights and similar entropic contributions (preexponentials) (Doster et al., 1982; Frauenfelder & Wolynes, 1985). This apparently would rule out the hypothesis derived from Agmon and Hopfield (1983).

However, these cryogenic kinetic analyses typically probe the photoproduct population surviving on time scales of several hundreds of nanoseconds and longer after photolysis. A strict accounting for the presence of unphotolyzed material is generally absent. For CO kinetic analysis, this is not a problem, since as we show here, and has been shown previously by us and others (Saffran & Gibson, 1977; Brunori et al., 1973; Noble et al., 1967; Chance et al., 1987; Ansari et al., 1987; Chance et al., 1983; Powers et al., 1987; Alben et al., 1982; Iizuka et al., 1974; Campbell et al., 1987), photolysis of CO bound to myoglobin at all temperatures is relatively complete; i.e., the observed photoproduct yield at short times and below 10 K exceed 95%. For O_2 photolysis, the situation at ambient temperatures is quite different.

In an attempt to address the origin of ligand-specific differences in photolytic yield and the origin of recombination differences between O_2 and CO, we have undertaken a transient absorption study with subnanosecond resolution of the photodissociation process at cryogenic temperatures. This study has measured the fraction of the total sample observed as photoproducts and the subnanosecond geminate recombination of photolyzed O_2 and CO ligands with hemoglobin and myoglobin from ambient to cryogenic temperatures. Using a combination of visible, near-infrared, and far-infrared absorption measurements, we have determined the 40-ps and long-time photoproduct yields at liquid helium temperatures for heme protein–ligand complexes. Finally, we examine to what extent the photolysis yields (both intrinsic and observed) are correlated with heme pocket structural parameters.

We show that for O_2 adducts, substantial quantities of material are either trapped in nondissociative states or recombine on ultrafast time scales. This poses a potential problem in the interpretation of the previous low-temperature kinetic data for O_2 and the contention that for MbO_2 and MbCO the distribution of barrier heights and the preexponential factors for recombination are similar (Frauenfelder & Wolynes, 1985).

Experimental Procedures

Picosecond transient absorption spectroscopy at low temperature was performed by using an actively/passively mode-locked Nd:YAG laser. The configuration is shown in Figure 1. A fraction of the frequency-doubled pulse (532 nm) was anti-Stokes Raman shifted in a hydrogen cell to provide the 436-nm probe pulse. This frequency was near the peak of the absorbance of the stable low-temperature photoproducts (see below). Cross-correlation of the 532-nm pump pulse and the 436-nm probe pulse was ≤40 ps, the average power was 220–250 mW at 532 nm, and the repetition rate was 10 Hz. A movable stage (Klinger) provided the optical delay between pump and probe. The probe beam was split near the sample and measured with a photodiode to provide a reference signal. The probe beam was spatially overlapped with the photolysis beam and directed through Janis liquid helium immersion Dewar to control the temperature of the sample. The output beam was detected with an identical photodiode, and the two

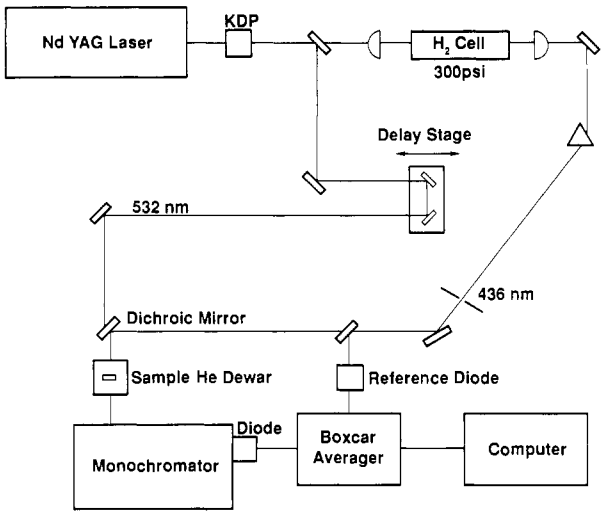

FIGURE 1: Diagram of picosecond transient absorption spectrometer. Details described in text.

diode outputs were ratioed with a Princeton Applied Research boxcar averager. The boxcar output was digitized and averaged in a computer. Data points for the picosecond transient experiments were taken every 100–200 ps with dwell times of between 2 and 5 s. Smoothed data were averaged in two separate regions, from +300 ps to +4 ns and from −500 ps to −100 ps using a mild Savitsky–Golay smoothing routine.

A large number of control experiments were carried out to establish the differences in behavior of the CO and O_2 low-temperature photoproducts. The photoproduct yields were determined on the basis of sample concentrations calculated from published and reverified extinction coefficients (at ambient and cryogenic temperatures) of the liganded material before photolysis (Antonini & Brunori, 1971; Srajer et al., 1986; Leone et al., 1987; Eaton et al., 1978). The results were based on dozens of measurements and many different preparations of Mb and Hb. No major inconsistencies among the various spectroscopic probes were found using this approach.

The extinction coefficient of the low-temperature Soret photoproduct band was required in order to correctly use the 436-nm single-wavelength probe to measure photoproduct concentrations. This extinction coefficient is not well established (Iizuka et al., 1974). A diode array spectrometer configuration described previously was used to measure liganded and photoproduct Soret spectra of MbCO and MbO_2 (Campbell et al., 1987). These spectra yielded the extinction coefficients at various wavelengths, allowing photoproduct yields to be calculated according to eq 1 where P^* = the

$$P^* = \log (I_0/I)(1/C)(1/cm)/(\epsilon_{pp} - \epsilon_L) \qquad (1)$$

photoproduct yield, I = the signal voltage, I_0 = the detector voltage at negative time on the optical delay stage for transient absorption experiments or voltage before any illumination for picosecond titration experiments, C = the sample concentration (millimolar), and cm = the path length of the sample; this was 0.158 cm for all the Soret measurements. Since 436 nm is close to the measured photoproduct peak, the observed voltages drop as the photoproduct concentration increases. ϵ_{pp} is the millimolar extinction coefficient of the photoproduct at 436 nm; ϵ_L is the millimolar heme protein–ligand extinction coefficient at 436 nm.

Since the CO samples were fully photolyzable, their ϵ_{pp} values could be observed directly with no correction for liganded material. The photoproduct peak was observed at 439 nm (Figure 2b), and the difference extinction coefficient, ϵ_{pp}

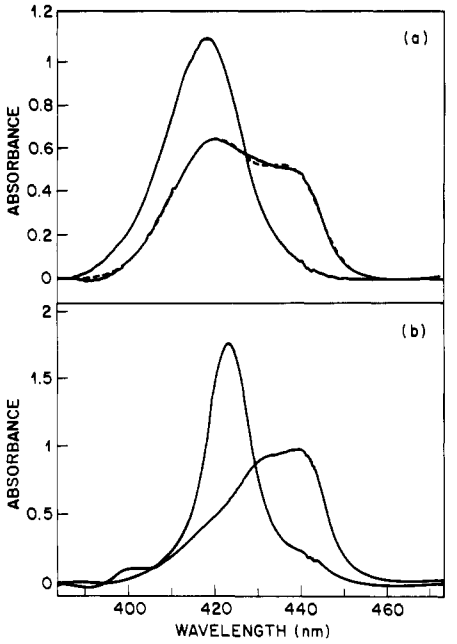

FIGURE 2: MbCO, MbO_2, and photoproduct spectra at 8 K. Spectra a are MbO_2 and its photoproduct (52 μM). Spectra b are MbCO and its photoproduct (61 μM concentration). Spectra shown are unsmoothed, and a cubic polynomial base line is subtracted from the data as described previously (Campbell et al., 1987). The photoproduct was generated by 15-min illumination from a tungsten projector. The peak of the MbCO photoproduct is at 439 nm. The MbO_2 photoproduct spectrum has at least two apparent components centered at 420 and 439 nm. The dashed line in spectra a is a two-Gaussian fit to the MbO_2 photoproduct spectra. The fit indicates a 42% loss of liganded material in the photoproduct.

$- \epsilon_L$, for MbCO at 436 nm and 8 K was estimated to be 78 ± 8 ODU mM^{-1} cm^{-1}. However, for MbO_2, it can be seen in Figure 2a that significant amounts of liganded material remain even after extended CW illumination sufficient to fully photolyze the MbCO sample. Other experiments at temperatures as low as 2 K did not alter the result. Therefore, since ϵ_{pp} for O_2 cannot be observed directly, we estimated its value from the loss of liganded material and the rise in the photoproduct band. The dashed line in Figure 2a represents a two-Gaussian fit with no parameters fixed to the MbO_2 photoproduct data. One Gaussian had a peak position equal to the position of the MbO_2-liganded band. The second Gaussian had a peak position at the frequency of the MbCO photoproduct band. The area and height of the first Gaussian corresponded to 58% of the fully liganded species. This implies that 42% of the sample remains photolyzed under these conditions. The height and area of the second Gaussian corresponded to 36% of the area and height of the 100% MbCO photoproduct peak. Therefore, the ϵ_{pp} for MbO_2 at 8 K must be very close to the value for MbCO; they are certainly equal within the errors of measurement. Assuming they are equal, $\epsilon_{pp} - \epsilon_L$ for MbO_2 at 436 nm and 8 K is estimated to be 99 ± 9 ODU mM^{-1} cm^{-1}. The difference at 436 nm for MbO_2 is greater than for MbCO because of the red shift of the MbCO peak compared to MbO_2. It is not possible with the present data to evaluate the possible changes in ϵ_{pp} as a function of temperture. Although the peak absorbancies of MbCO and MbO_2 vary somewhat with temperature from 10 to 150 K, the effects at 436 nm are negligible compared to other uncertainties. Thus, we feel that these difference extinction coefficients can be applied to all the transient absorption data seen in the paper.

In order to confirm that the single-wavelength absorbance data from the picosecond transient absorption experiments

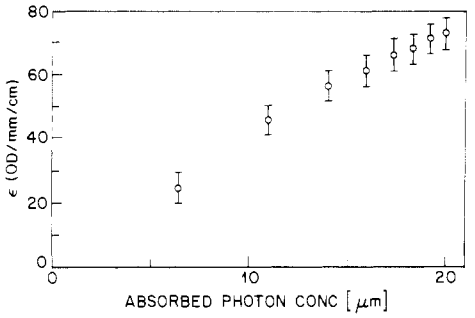

FIGURE 3: Picosecond titration of a HbCO sample of 21 μM. Each point represents additional single pulses of a the 532-nm picosecond laser at 15-mW average power. This represents a photon concentration of 53 μM per pulse. Considering the sample OD at the pump wavelength, 6.4 μM photon is absorbed by *liganded* states in the first pulse. The absorbance change (extinction) is calculated at the 436-nm probe wavelength, which was so weak as to not photolyze the sample. The liganded material remaining after a pump pulse is calculated from the absorbance change at the 436-nm probe wavelength, and the absorbed photon concentration for the next pump pulse at 532 nm is calculated based only on 532-nm absorption by liganded states. This process is repeated for each pulse, so that the absorption contribution of photoproduct states is subtracted out in the calculation of absorbed photons. The *x* axis represents the net photon concentration absorbed by liganded states only. The sample reaches 95% photolysis when 95% of the liganded states have been interrogated (20 μM absorbed photon concentration). Subsequent multiple flashes increase the extinction to the Soret calculated value of 78.

agreed with the Soret data, we carried out a number of phototitration experiments with 40-ps pulses. Representative results are seen in Figure 3. Phototitration experiments were performed by measuring the absorbance changes at 436 nm and 8 K pulse by pulse, i.e., titrating the absorbance changes. Initial experiments simply compared the probe 436-nm detector voltages before illumination and after a large number (100 or more) of 532-nm photolyzing pulses for various MbCO, MbO_2, HbCO, and HbO_2 samples at 8 K. This consistently gave photoproduct yields close to those of the Soret experiments carried out with myoglobin. In Figure 3, we show a careful titration of the absorbance changes in order to simultaneously test the conjunction of power measurements, sample concentrations, path lengths, and detector linearity. The total absorbance change at the pump wavelength is small, since the photoproduct and liganded absorbance are within 20%.

One feature of such a titration is that photon absorption by already photolyzed molecules does not further contribute to increases in the photoproduct yield. As such, typical titration curves show successively smaller increases in 436-nm probe absorbance with every flash. For Figure 3, we calculated the remainder of liganded material after each pump pulse, and therefore the *x* axis represents the net concentration of photons absorbed *only* by liganded states. The result is plotted against the total absorbance (extinction) of the sample at 436 nm. The linear result shows that for each pulse, the production of photolyzed states (absorbance increase) is directly proportional to the number of liganded species which absorb photons (in the limit of low concentration). If the ordinate axis is transformed into the concentration of photolyzed HbCO by use of our calculated extinction coefficients, the slope of the line in this experiment is close to 1. Each liganded molecule needs absorb only one photon to become photolyzed. If the slope of the line was substantially less than 1, this would imply that it requires a multiphoton process to generate the MbCO photoproduct state. This establishes that optical pumping into long-lived states is not a major component of the conversion to stable photoproducts. Figures 2 and 3 represent a fraction

Table I: Stable Photoproduct Yields of Hemoglobin and Myoglobin at 8 K after CW Photolysis[a]

sample	Soret	760 nm	far-IR (1950 cm^{-1})
horse MbCO	1.0 ± 0.1	0.95 ± 0.05	0.95 ± 0.05
human HbCO	1.0 ± 0.1	0.90 ± 0.1	N/A
horse MbO_2	0.4 ± 0.1	0.45 ± 0.05	N/A
human HbO_2	0.4 ± 0.1	N/A[b]	N/A

[a] The rows represent the sample type; the columns represent the spectral region used to measure the yield. [b] N/A, not yet available.

of the control experiments carried out to ensure the accuracy of the results.

The transient absorption experiments used a range of photons per molecule with no significant changes in the results. Near-infrared spectra (760 nm) were taken with a diode array spectrometer as described previously (Campbell et al., 1987). Near-IR spectra were normalized by fitting a cubic polynomial to the blue and red edges of the spectrum removed from the 760-nm absorption band. This curve corresponds to the tail of the visible absorption band and was subtracted from the near-IR data. FT-IR spectra data are from Chance et al. (1987).

Horse myoglobin was prepared according to standard methods (Antonini & Brunori, 1971) and human hemoglobin, the A_0 form, was the gift of Dr. Robert Noble. All samples contained 50 mM potassium phosphate buffer (pH 7.5) and 75% glycerol.

Results

We calculated the stable quantum yields of photolysis for oxy and carbonmonoxy complexes using three different spectroscopic markers at 8 K (Table I). All the samples were photolyzed with CW light; then the light was extinguished and an appropriate weak probe light was used to examine the spectra. All these values represent the stable or "permanent" yield. The Soret column includes the permanent yield with CW light as ascertained with "full" spectra, as seen in Figure 2a,b, and the permanent yield after multiple flashes of the 532-nm laser, using a 436-nm probe, as in Figure 3. The results were identical within the errors. The yield of stable photoproducts was 90–100% for MbCO and HbCO with each technique. The spectroscopic markers used included a liganded mode undisturbed by deoxy markers (far-IR), a deoxy absorption band distinct from any liganded influences (near-IR), and the Soret region, where liganded and deoxy absorption bands overlap. The results for MbO_2 and HbO_2 showed considerably less photolysis, averaging 40–45% when three kinds of measurements (diode array and single wavelength in the Soret and near-IR) and two different spectroscopic markers were used.

The subnanosecond kinetics of rebinding for photolyzed HbO_2 and HbCO showed little variation between room temperature and 150 K. For photolyzed HbO_2, 60% of the Soret absorption at 436 nm decays within 2 ns. By comparison, HbCO exhibits only 10–15% recombination on this time scale. Comparable measurements on MbO_2 proved difficult in that the sample stability at the higher temperatures was lower; nonetheless, it is clear that photolyzed MbO_2 shows much less subnanosecond recombination than HbO_2. The MbCO samples showed little recombination over the 2-ns time frame.

In Figure 4, the geminate recombination for HbO_2 and HbCO is shown at 150 K. The 75% glycerol sample is frozen, and the sample fully recombines within 0.1 s. The figure shows the raw absorbance changes, using the sample concentration, path lengths, and difference extinction coefficients; the pho-

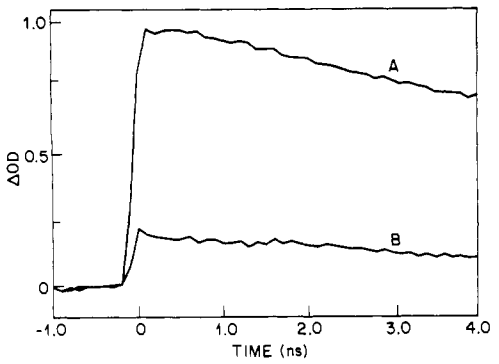

FIGURE 4: Picosecond transient absorption spectra of HbCO and HbO_2 at 150 K. Average laser power is 50 mW. The O_2 sample (curve B) is 150 μM, and the CO sample is 130 μM (curve A). Data are unsmoothed.

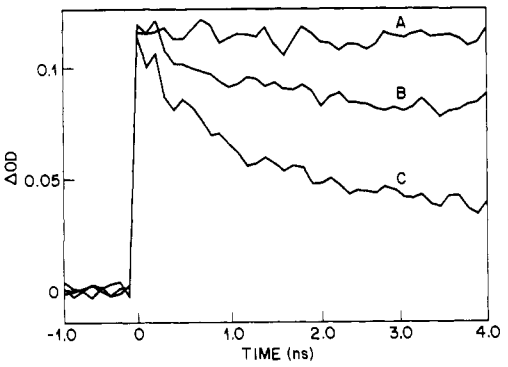

FIGURE 5: Temperature dependence of geminate recombination for HbO_2. Laser power is 15 mW; sample concentration is 137 μM. Data are smoothed as described. Considering the concentration of absorbed photons per pulse (30 μM), an extinction of 24 ODU mM^{-1} cm^{-1} or a photoproduct yield of 0.25 ± 0.1 is indicated for these experiments. Curve A, 70 K; curve B, 100 K; curve C, 150 K.

toproduct yield at 50 ps for the HbO_2 sample is 0.2 ± 0.1; for the CO sample, it is 1.0 ± 0.1 (see other figures for representative calculations). Figure 4 clearly shows significant differences in absorbance jump and photoproduct yield for two samples of equal concentration at identical laser powers. To minimize the experimental differences, we used a double cell with an O_2 sample mounted directly above a CO sample in the Dewar. The two samples could be moved vertically to bring one or the other into the beam in a matter of seconds for experiments closely spaced in time. This minimized any changes in temperature or laser power. The results consistently showed these relative differences for HbO_2 compared to HbCO. The fast phase of geminate recombination for HbO_2 at 150 K shows that approximately 60% of the absorbance at 436 nm has decayed within 2 ns, similar to results at 250 K (Friedman et al., 1985). Fits to single exponentials were unsuccessful, double-exponential fits were quite good, but the longer lifetime was above 2 ns. More decades in time are needed to adequately analyze the kinetic parameters. However, it is clear that at 150 K, the photoproduct yield for HbO_2 at *2 ns* is 0.08 or less, while for HbCO it is effectively 0.85 (15% has recombined). Thus, the nanosecond photoproduct yield for HbO_2 begins to approach the microsecond yields of approximately 0.03.

These geminate processes for HbCO and HbO_2 are relatively unaffected by temperature in the range 190–150 K, and the observed curves are overlapping. From 150 to 70 K, the rate of geminate recombination for HbO_2 decreases significantly while the absorbance jump remains constant. Figure 5 shows experiments at 150, 100, and 70 K. Clearly, the fast geminate process is reduced at 100 K and is absent at 70 K.

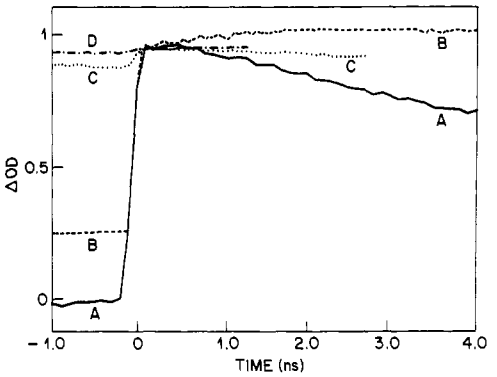

FIGURE 6: Temperature dependence of HbCO geminate recombination. Samples are 130 μM; laser power is 50 mW average. Data are unsmoothed. Curve A, 150 K; curve B, 70 K; curve C, 40 K; curve D, 20 K. Considering the concentration of absorbed photons per pulse (74 μM), an extinction of 81 ODU mM^{-1} cm^{-1} or a photoproduct yield of 1.0 ± 0.1 is implied for this experiment.

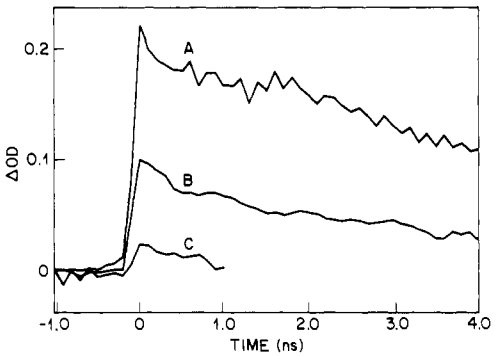

FIGURE 7: Power dependence of HbO_2 geminate recombination at 150 K. Curve A, 50 mW; curve B, 15 mW; curve C, 5 mW average power. Sample concentration is 154 μM; data are smoothed as described. The transient absorbance changes across zero time taking into account the different laser powers and numbers of absorbed photons are 16, 24, and 17 ODU mM^{-1} cm^{-1} for curves A, B, and C, respectively.

At or below 70 K, HbO_2 recombination resembles HbCO geminate recombination (see below).

In Figure 6, the temperature dependence of the HbCO recombination is shown. At temperatures lower than 90 K, the overall recombination rate slows to the extent that some of the molecules do not recombine before the next laser pulse. Thus, the "baseline" absorbance in the transient absorption experiment rises with decreasing temperature, while the absorbance jump across zero time drops. Curve 6B shows the beginnings of this process. At 20 K (curve 6D), the absorbance jump is very small, and the base line is correspondingly high since 90% of the sample does not recombine within 0.1 s.

Figure 7 shows the power dependence of the picosecond geminate recombination of HbO_2 at 150 K. The absorbance jump scales with the number of absorbed photons, and the kinetics are similar regardless of the power. Similar experiments with HbCO also showed no variations in the kinetics at different powers.

For HbCO, the photoproduct yield data indicate that at very low temperature (8 K), 90–100% of the sample can be converted to photoproducts that do not recombine between laser pulses. This implies that one should not observe a significant absorbance jump across zero time at this temperature when the delay stage is scanned, since the sample is fully photolyzed or pumped by the 10-Hz laser. We find that when the stage is scanned across zero time, no significant change in absorbance is observed for both HbCO and MbCO. For HbO_2 and MbO_2, the photoproduct yield (at 8 K) is on the order of 40%

so that 60% or more of the sample is *unphotolyzed*. Here, the absorbance jump across zero time is on the order of 5%, but no recombination is observed out to 4 ns. Therefore, this 5% fraction recombines between 4 ns and 0.1 s. A large fraction of the sample apparently recombines (or does not photolyze) within the pulse duration. Variations in laser power did not change the result. These results show that the *observable* photoproduct population of MbO_2 recombines slightly faster than that of MbCO, consistent with earlier observations (Doster et al., 1982).

For HbCO and MbCO, we achieved complete photolysis both at long times and low temperatures (8 K) and at short times (40 ps) and higher temperatures. For O_2, the results were quite different. At 150 K, 80% of the MbO_2 and HbO_2 samples do not appear as photoproducts after 40-ps laser pulses. For HbO_2, the 20% that does appear as photoproduct undergoes temperature-dependent recombination. As the temperature is dropped, for O_2 samples the yield of stable photoproducts rises, so that at 8 K, close to 40% of the MbO_2 and HbO_2 samples appear as photoproducts. At 8 K for O_2, 5% of the population recombines within 0.1 s, while for CO <5% recombines.

Discussion

Photoproduct Yields at Cryogenic Temperatures. Previous solution-phase picosecond transient absorption studies on hemoglobin using photolysis pulses of 30-ps duration have demonstrated that whereas CO undergoes little geminate recombination within the first few nanoseconds of photolysis, O_2 exhibits a substantial geminate phase over several hundred picoseconds (Freidman et al., 1985). In the present study, the above oxy/carbonmonoxy difference is observed not only for room temperature solution-phase samples but also for frozen samples well below 200 K. This persistence in the pattern of subnanosecond geminate recombination for the HbO_2 samples even at 150 K is significant for several reasons. At cryogenic temperatures, the observation of distributed kinetics and kinetic hole burning has supported the idea of conformational subtates (Austin et al., 1975; Doster et al., 1983; Ansari et al., 1985; Campbell et al., 1987; Agmon et al., 1988). These states represent distinct molecular species that interconvert only slowly at these temperatures. They are distinct, and react with distinct rate constants, because of differences in atomic coordinates that are responsible for controlling the rebinding. Below 180 K, escape of ligands from the vicinity of the heme pocket ceases (Austin et al., 1975; Ansari et al., 1986). Recombination at this temperature and below is exclusively from within the protein, and consequently, the kinetics should be dominated by this quasi-frozen distribution of conformations and energy barriers. The observation of this subnanosecond rebinding process in HbO_2 down to 150 K shows (1) that this rebinding is clearly from within the heme pocket and (2) the relevance of these cryogenic studies to room temperature processes.

The kinetic data of Frauenfelder and co-workers (Austin et al., 1975; Alberding et al., 1978; Doster et al., 1982; Ansari et al., 1985) suggest that their process I, recombination from within or near the heme pocket, for CO and O_2 recombination is similar but exhibits measurable although not substantial differences in the average barrier to recombination and the distribution shape (Doster et al., 1982). Our results demonstrate processes that are drastically different in CO and O_2 rebinding, requiring a reexamination of these earlier conclusions.

The yield of photoproducts at 40 ps for HbO_2 and MbO_2 is consistently less than unity at all temperatures between 200 and 2 K. It is important to understand the reasons why such a fast recombining or unphotolyzable population is present for O_2 ligands but absent for CO. Although there are difficulties in comparing the absolute absorbance changes for frozen samples of this type, the consistently of the results and the large differences observed umambiguously indicate significant differences between the ligands. Clearly, the full distribution of carbonmonoxy heme protein substates contributes to the measured properties of the photoproduct, whereas only a fraction of the oxy population is contributing.

A key question is to what extent is the apparently less than unity quantum yield for the oxy derivatives either a function of the intrinsic yield or due to picosecond or faster recombination events. Further, considering the existence of conformational substates at cryogenic temperatures; (a) does each distinct state have a fixed probability of photodissociating when illuminated, or (b) is the intrinsic yield a distinct feature of each molecule determined by its conformation, or (c) is the yield for each and every substate unity and a fraction of the molecules are in conformational substates that experience essentially no barrier to recombination, so that they can recombine within a 40-ps pulse duration at 8 K? Possibility (a) seems to be ruled out by the absence of significant pumping of the sample at low temperature. If there were simply a fixed probability of being photolyzed into a stationary state, ultimately the entire sample would become photolyzed. Possibilities (b) and (c) remain the important ones to distinguish. The present results suggest that possibility (c) is the most viable model.

From 190 to 70 K, the photoproduct yield (0.2) is unchanged for HbO_2, while the subnanosecond recombining population decreases significantly. Further decreases in temperature to 8 K result in a doubling of the photoproduct yield to 0.4. Eighty percent of the sample population was not observed as photoproduct at 70 K and above; however, the kinetics of some portion of these "unphotolyzable" states have been slowed into the observed photoproduct population at 8 K. Therefore, a portion of the "unphotolyzable" population is clearly photolyzable, and the temperature-dependent recombination of this fraction accounts for the rise in photoproduct yield to 0.4 at 8 K. For MbCO and HbCO below 10 K, essentially the entire population is converted to stable photoproducts, whereas for HbO_2 and MbO_2 ca. 55% is unphotolyzable (with 40-ps pulses), 5% recovers between pulses, and 40% is stable photoproduct. Previous observations (Petrich et al., 1988), that subpicosecond recombination is significant for oxyheme protein species, support the idea that the differences in observed yield may be entirely due to ultrafast relaxation. However, the data here suggest that relaxation from an electronically excited geminate pair is not the full explanation for the observed O_2 yields, unless this relaxation is temperature dependent. At the very least, these results provide no direct evidence for differences in the intrinsic yield.

Our results are apparently at odds with the data of Valat and Alpert (1985), who measured the 30-ps quantum yield of HbO_2 as 0.65 ± 0.15. We believe they have overestimated the 30-ps yield since there are several problems with their calculation. They base their quantum yield determination on the slope of a plot of OD change versus laser power at low power levels. Although this is reasonable in principle, in this case it is subject to several errors. One problem, they admit, is that the true Hb spectrum of the deligated species is not known. This is a problem for our analysis also, although we can measure the low-temperature photoproduct directly. Another is the lack of consideration of the overlap of the deoxy

and liganded absorbance at the probe wavelength of 576 nm. Unfortunately, the slope of the power curve at both low light levels and small absorbance changes in subject to quite large errors. However, closer examination of their raw data shows some agreement with our results. They show a power curve demonstrating the saturation of OD changes with increasing power; the maximum OD change can be read off their curve. Using this OD value, their path length and concentration, and estimating the difference extinction coefficient at 576 nm based on room temperature deoxy and liganded spectra (Antonini & Brunori, 1971), we calculate a photoproduct yield value of 0.36 ± 0.15, equal to our result of 0.2 ± 0.1 at 150 K within the error.

Another feature of the results to be considered is the invariance of the photolytic yield from 190 to 70 K. One mechanism which could make the absorbance jump constant in this region would involve a fraction of the sub-40-ps recombining states slowing into the nanosecond regime while an equal fraction of nanosecond recombining states slows out of the observation window. Since the entire sample recovers between pulses in this range, we have no data to demonstrate this. If this is true, then nanosecond to millisecond recombination data should reflect it. In summary, for both MbO_2 and HbO_2, subpicosecond processes contribute to the lower microsecond yields observed compared to CO adducts at all temperatures. In addition, the subnanosecond geminate recombination for HbO_2 is substantial even at 150 K.

Ligand Specificity of Recombination Kinetics. Previous studies by Doster et al. (1982) and Frauenfelder and Wolynes (1985) have determined that the barriers to the heme for O_2 and CO are quite similar. The preexponentials and the peak activation enthalpies of MbCO differ from those of MbO_2 by less than 10%. This was reasonably considered surprising, since the free ligands are quite different electronically. The preexponentials, on the order of 10^9, were substantially lower than the canonical value of 10^{12}. This was not necessarily considered evidence of nonadiabaticity, since entropy losses on binding and frictional forces can also reduce the preexponential. The general conclusion was that the electronic differences in the ligand rebinding were overcome by steric factors in the protein that rendered the observed binding similar (Frauenfelder & Wolynes, 1985). The results presented here are inconsistent with these conclusions.

The picosecond geminate recombination of HbO_2 is a process with a rate on the order of 5×10^9 s^{-1}. The subpicosecond recombination seen for both MbO_2 and HbO_2 is even faster. Thus, a fixed preexponential value of 10^9 is inconsistent with processes this fast. Therefore, these subnanosecond and subpicosecond processes cannot be an extension of the 10^9 preexponential process I of Frauenfelder and co-workers to faster times than previously observed (Doster et al., 1982; Ansari et al., 1985). If the 10^9 preexponential is adjusted upward, then the estimated barrier heights of Doster et al. (1982) will necessarily change. Following this line of reasoning, it could then be imagined that the ultrafast geminate processes we observe represent the lower barrier edge of the process I distribution. That is, with a preexponential of 10^{10} and a barrier height of 0.2 kcal/mol at 150 K, the implied rate is reasonable. However, this still cannot account for the fact that 60–80% of the O_2 population at all temperatures recombines within 40 ps and that the subnanosecond geminate process for HbO_2 at 150 K recombines 60% of the surviving photoproducts. This makes it difficult to preserve the process I barrier shape and size.

Our results do support the idea that the photoproduct populations for O_2 and CO observed by Doster et al. (1982) are similar, with O_2 rebinding slightly faster. For example, at 8 K, the presence of an absorbance jump of 5% for the MbO_2 sample compared to <5% for the MbCO sample in the transient absorption experiments indicates that the observed MbO_2 photoproduct population is slightly faster as previously observed. Our concern is with the significant fraction of the population not observed by these previous experiments.

Another factor distinguishing the O_2 kinetics from that of process I is the temperature dependence of the picosecond rebinding phase. The picosecond geminate recombination of HbO_2 has similar kinetic curves in the region from 190 to 150 K. The origins of this apparently non-Arrhenius behavior are unclear. The fast phase is lost in a gradual transition from 140 to 80 K, and is completely gone at 70 K. The temperature dependence of process I in no way resembles these results. In addition, if this process did represent the low barrier edge of process I, it would show significant and continual slowing in the region 190–70 K. The temperature dependence of this phase indicates that the rebinding structures must be altered as the temperature drops.

Previously, we and others have observed significant kinetic and spectroscopic changes in heme proteins centered at 100 K (Powers et al., 1987; Campbell et al., 1987; Agmon, 1988). For example, from 8 to 100 K, the proximal histidine stretching frequency of deoxymyoglobin and its photoproducts is invariant; above 100 K, it begins to shift to the room temperature equilibrium deoxy value, and the shift is complete by 180 K (Powers et al., 1987). Agmon (1988) has also observed a "kink" in the temperature dependence of the near-infrared recombination data of Ansari et al. (1985). This transition may be indicative of the onset of structural relaxation processes contributing to frequency shifts in the near-infrared band. We have previously observed that structural relaxation monitored by this near-infrared absorption band is not observed below 60 K (Campbell et al., 1987) and probably is also minimal below 100 K. Friedman et al. (1985) have shown that the fast geminate phase of O_2 kinetics is solvent and protein structure dependent. There obviously is a transition region where the temperature begins to slow the fast geminate phase. We speculate that specific degrees of freedom related to the proximal histidine and control of iron displacement are frozen out in this temperature region. In summary, a substantial fraction of the O_2 photoproduct population is distinct from the process I described by Frauenfelder and co-workers, while the photoproducts surviving beyond 4 ns clearly recombine by a process I mechanism.

Ligand Specificity of Initial Photodynamics. Petrich et al. (1988), using femtosecond time-resolved absorption studies at room temperature, found evidence for ligand-specific variations in the proportion of excited states that evolved into either the starting liganded material or the fully dissociated deoxy-like photoproduct. Excited-state photophysics may be partially responsible for ligand-specific differences in observed photoproduct yields. If the branching ratio is the same for all substate conformations, then continued photolysis of O_2 adducts would drive the photolytic yield toward unity at 8 K since they would be trapped once photolyzed. Our results indicate that if branching ratios are present at cryogenic tempertures, they are a strong function of substate structure, with some structures predisposed toward the pathway leading to ground-state recovery, while other structures are predisposed toward the pathway leading to stable photoproducts. Essentially, if branching ratios of electronic excited states are im-

portant to quantum yields, they are strongly correlated to heme protein structure.

It is reasonable that the proximal heme pocket configuration, both the iron displacement and the histidine configuration, could modulate branching ratios for different ligands through the energies and dynamics of the relevant short-lived excited electronic states. Alternatively, the nonphotolyzing population reflects conformational states having essentially a zero barrier for recombination. Such a barrierless population would appear nonphotolyzable due to ultrafast recombination. Agmon and Hopfield (1983) have asserted that the full distribution of rebinding rates includes some fraction of substates undergoing barrierless recombination. For O_2 rebinding, the fraction is seemingly quite large. It remains to be established what role the proximal heme pocket and iron displacement have in these photoproduct yield and reactivity differences.

Both X-ray crystallographic (Baldwin & Chothia, 1979; Dickerson & Geis, 1983; Perutz et al., 1987) and X-ray absorption studies (Chance, 1986; Chance et al., 1986) have shown that in the equilibrium structures of MbO_2 and MbCO, the iron is ca. 0.2 Å out of the heme plane in MbO_2 and close to the plane of the heme for MbCO. The deoxy species are well established as having a significantly displaced iron (0.4–0.5 Å). Soret studies by Srajer et al. (1986) and both X-ray and Mossbauer studies indicate that the iron coordinate in deoxy forms is significantly distributed (Frauenfelder et al., 1979; Parak et al., 1984). For the 4 K MbCO photoproduct, the iron moves to 75% of its equilibrium deoxy displacement (Chance, 1986; Chance et al., 1986; Powers et al., 1987). Srajer et al. (1988) have used this value to successfully simulate the low-temperature data of Austin et al. (1975). In this model, the photolyzed population is represented by a distribution of iron displacements centered at 0.35 Å; states with increased iron displacement have a higher proximal barrier to recombination. Campbell et al. (1987) demonstrated that the 760-nm band III of photodissociated MbCO, which is assigned as an $a_{2u}(\pi)$–d_{yz} transition, is inhomogeneously broadened by a distribution of substates. The substate population with lower barriers to recombination comprises the red edge of band III. More recently, Chavez et al. (1990) demonstrated correlations between the behavior of proximal sensitive resonance Raman bands and band III in a variety of T- and R-state hemoglobins. Band III is strongly correlated with the proximal heme pocket; therefore, a distribution of proximal histidine structures and iron displacements is correlated with reactivity.

This suggests a possible explanation for the relationship between the slower and faster O_2 rebinding phases, the similarity of CO rebinding with the slower phase of O_2, and the meaning of the preexponential term. The small (10^9) preexponential for rebinding can be rationalized in terms of large frictional forces or large entropy losses on binding (Frauenfelder & Wolynes, 1985). If the entropy changes for CO and O_2 binding are similar, then differences in frictional forces may account for the differences in O_2 reactivity. For the MbCO photoproduct, it is possible that virtually all the substates would experience such frictional forces opposing rebinding, since the iron must move fully in plane for rebinding. For O_2 photolyzed states where iron is substantially out of plane, similar frictional forces would obtain, and this fraction of the population would also have a lower preexponential (10^9). O_2 photoproduct states that have iron relatively close to the liganded position of 0.2 Å will exhibit substantially less friction upon rebinding. Therefore, a larger preexponential for this subpopulation is not unreasonable.

For MbCO at pH 3, the proximal histidine–iron bond is cleaved, and the frictional forces opposing rebinding should be low. Using picosecond time-resolved Raman studies, it can be seen that a substantial fraction of the pH 3 MbCO recombines within picoseconds of photodissociation (I. Iben, B. Cowen, and J. Friedman, unpublished observation). Apparently, a significant fraction of the molecules have very fast rebinding.

This analysis centers on control by the proximal side; however, O_2 rebinding is also influenced by distal interactions. It is well accepted that O_2 hydrogen bonds to a water molecule or the histidine in the distal pocket; this may also be involved in the differences observed between O_2 and CO reactivity (Kitagawa et al., 1982; Dickerson & Geis, 1983). Jongeward et al. (1987) have observed differences in the geminate recombination of MbCO and MbO_2, with MbO_2 exhibiting a faster rebinding phase as seen here. However, they conclude that the rebinding differences are related to the trajectory of the photolyzed ligand. For the slower rebinding phase, the ligand "wanders" in the heme pocket.

Recently, Postlewaite et al. (1988) have shown that in the absence of proximal strain CO exhibits substantial recombination with protoheme on the picosecond time scale over a wide variety of temperatures. This process is apparently very small or absent for protein–CO reactions since we observe a photoproduct yield of 1.0 at 40 ps. The actual photoproduct yield in the measurements of Postlewaite et al. is unclear; however, the absence of an ultrafast processes for protein–CO complexes is suggestive of an inhibitory role for the protein relative to ultrafast CO recombination in protoheme. This inhibitory role may be the frictional forces alluded to above, lowering the preexponential in the protein–CO reactions. Apparently, the proximal heme pocket plays a key role in determining the barrier for CO recombination. Since O_2 may recombine more easily to a nonplanar heme, low-barrier or barrierless recombination is more probable than for CO–protein complexes.

Conclusion

Prior nanosecond and longer kinetic experiments reporting MbO_2 and HbO_2 recombination at cryogenic temperatures essentially probed only a small part of the kinetic distribution. At and above 150 K, for HbO_2, the 40-ps photoproduct yield is 0.2. Since 60% of these observed photoproducts recombine within 2 ns, the fraction of molecules recombined on nanosecond time scales is over 90%. For MbO_2, where there is less subnanosecond geminate recombination, the fraction of recombined species at 150 K and 2 ns is closer to 80%. Also, the recombination rates and the temperature dependence of this O_2 phase clearly have different parameters than process I described by Frauenfelder and co-workers. This phase represents the major pathway for O_2 recombination at low temperatures and dictates the heme barrier for O_2. In this light, we have reexamined the conclusions of low-temperature kinetic data on O_2 recombination and its relationship to CO recombination. Essentially the longer time *observed* populations recombine similarly; however, a large fraction of the O_2 population recombines by a different pathway or mechanism, which apparently is linked to the frictional forces of the proximal heme pocket. We have shown that CO and O_2 low-temperature recombination kinetics are fundamentally different due to both subnanosecond and subpicosecond kinetic events which favor O_2 rebinding. Since CO is essentially a poisonous ligand, this may be an important kinetic mechanism for distinguishing between the two. The mechanistic basis for this discontinuity in the recombination processes between O_2 and CO rebinding is essential to the understanding of the

molecular reactivity and recognition processes of globin proteins. We have attempted to quantitate the rudimentary features of the differences between these ligands in the hope that it will stimulate further study of the origin of this reactivity behavior.

References

Agmon, N. (1988) *Biochemistry 27*, 3507–3511.

Agmon, N., & Hopfield, J. (1983) *J. Chem. Phys. 79*, 2042.

Alben, J. O., Beece, D., Bowne, S. F., Doster, W., Eisenstein, L., Frauenfelder, H., Good, D., McDonald, J. D., Marden, M. C., Moh, P. P., Reinisch, L., Reynolds, A. H., Shyamsunder, E., & Yue, K. T. (1982) *Proc. Natl. Acad. Sci. U.S.A. 79*, 3744–3748.

Alberding, N., Chan, S., Eisenstein, L., Frauenfelder, H., Good, D., Gunsalus, I., Nordlund, T., Perutz, M., Reynolds, A., & Sorensen, L. (1978) *Biochemistry 17*, 43–51.

Alpert, B., Mohsni, S. E., Lindqvist, L., & Tfibel, F. (1979) *J. Chem. Phys. 64*, 11–16.

Ansari, A., Berendzen, J., Bowne, S. F., Frauenfelder, H., Iben, I. E. T., Sauke, T. B., Shyamsunder, E., & Young, R. D. (19856) *Proc. Natl. Acad. Sci. U.S.A. 82*, 5000–5004.

Ansari, A., Dlott, D. D., Frauenfelder, H., Iben, I. E. T., Langer, P., Sauke, T., & Shyamsunder, E. (1986) *Biochemistry 25*, 3139–3146.

Ansari, A., Berendzen, J., Braunstein, D., Cowen, B. R., Frauenfelder, H., Hong, M. K., Iben, I. E. T., Johnson, J. B., Ormos, P., Sauke, T. B., Scholl, R., Schulte, A., Steinbach, P. J., Vittitow, J., & Young, R. D. (1987) *Biophys. Chem. 26*, 337–355.

Antonini, E., & Brunori, M. (1971) *Hemoglobin and Myoglobin in Their Reactions with Ligands*, North-Holland, Amsterdam.

Austin, R. H., Beeson, K., Eisenstein, L., Frauenfelder, H., & Gunsalus, I. C. (1975) *Biochemistry 14*, 5355–5373.

Baldwin, J., & Chothia, C. (1979) *J. Mol. Biol. 129*, 175–200.

Brunori, M., Giacometti, C., Antonini, E., & Wyman, J. (1973) *Proc. Natl. Acad. Sci. U.S.A. 70*, 3141–3144.

Campbell, B. C., Chance, M. R., & Freidman, J. M. (1987) *Science (Washington, D.C.) 38*, 373–376.

Chance, B., Fischetti, R., & Powers, L. S. (1983) *Biochemistry 22*, 3820–3829.

Chance, M. R. (1986) Ph.D. Thesis, University of Pennsylvania, Philadelphia, PA.

Chance, M. R., Parkhurst, L. J., Powers, L. S., & Chance, B. (1986) *J. Biol. Chem. 261*, 5689–5692.

Chance, M. R., Hoover, R., Campbell, B. C., & Friedman, J. M. (1987) *J. Biol. Chem. 262*, 6959–6961.

Chavez, M. D., Courtney, S., Chance, M. R., Kiula, D., Nocek, J., Hoffman, B. M., Friedman, J. M., & Ondrias, M. R. (1990) *Biochemistry 29*, 4844–4852.

Chernoff, D. A., Hochstrasser, R. M., & Steele, A. W. (1980) *Proc. Natl. Acad. Sci. U.S.A. 77*, 5606–5610.

Cornelius, P. A., Hochstrasser, R. M., & Steele, A. W. (1983) *J. Mol. Biol. 163*, 119–128.

Dickerson, R. E., & Geis, I. (1983) *Hemoglobin Structure, Function, Evolution, and Pathology*, p 51, Benjamin Cummings, Menlo Park, CA.

Doster, W., Beece, D., Bowne, S. F., DiIorio, E. E., Eisenstein, L., Frauenfelder, H., Reinisch, L., Shyamsunder, E., Winterhalter, K. H., & Yue, K. T. (1982) *Biochemistry 21*, 4831–4839.

Duddel, D. A., Morris, R. J., & Richards, J. T. (1979) *J. Chem. Soc., Chem. Commun.*, 75–80.

Eaton, W. A., Hanson, L. K., Stephens, P. J., Sutherland, J. C., & Dunn, J. B. (1978) *J. Am. Chem. Soc. 100*, 4991–5003.

Frauenfelder, H., & Wolynes, P. G. (1985) *Science 229*, 337–345.

Frauenfelder, H., Petsko, G., & Tsernoglou, D. (1979) *Nature (London) 280*, 558–563.

Friedman, J. M., & Lyons, K. B. (1980) *Science 284*, 570–572.

Friedman, J. M., Scott, T. W., Fisanick, G. J., Simon, S. R., Findsen, E. W., Ondrias, M. R., & Macdonald, V. R. (1985) *Science 229*, 187–191.

Gibson, Q. (1959) *Biochem. J. 71*, 293–303.

Gibson, Q., & Ainsworth, S. (1959) *Nature 180*, 1416–1417.

Gibson, Q., & Antonini, E. (1967) *J. Biol. Chem. 242*, 4678.

Hofrichter, J., Sommer, E., Henry, E., & Eaton, W. A. (1983) *Proc. Natl. Acad. Sci. U.S.A. 80*, 2235.

Iizuka, T., Yamamoto, H., Kotani, M., & Yonetani, T. Y. (1974) *Biochim. Biophys. Acta 371*, 126–139.

Jongeward, K. A., Magde, D., Taube, D., Marsters, J. C., Traylor, T. G., & Sharma, V. (1987) *J. Am. Chem. Soc. 110*, 380–390.

Leone, M., Cupane, A., Vitrano, E., & Cordone, L. (1987) *Biopolymers 26*, 1769–1779.

Martin, J. L., Mingus, A., Poyart, A., Lecarpinter, T., Antonelli, A., & Orszag, A. (1983) *Proc. Natl. Acad. Sci. U.S.A. 107*, 803–810.

Noble, R., Brunori, M., Wyman, J., & Antonini, E. (1967) *Biochemistry 6*, 1216–1222.

Parak, F., & Knapp, E. (1984) *Proc. Natl. Acad. Sci. U.S.A. 81*, 7088–7092.

Perutz, M. F., Fermi, G., Luisi, B., Shaanan, B., & Liddington, R. C. (1987) *Acc. Chem. Res. 20*, 309–321.

Petrich, J. W., Poyart, C., & Martin, J. L. (1988) *Biochemistry 27*, 4049–4060.

Postlewaite, J., Miers, J., & Dlott, D. (1988) *J. Am. Chem. Soc. 111*, 1248–1255.

Powers, L. S., Chance, B., Chance, M. R., Campbell, B. F., Friedman, J. F., Khalid, S., Kumar, C., Naqui, A., Reddy, K. S., & Zhou, Y. (1987) *Biochemistry 26*, 4785–4796.

Saffran, W., & Gibson, Q. H. (1977) *J. Biol. Chem. 252*, 7955.

Srajer, V., Schomaker, K., & Champion, P. (1986) *Phys. Rev. Lett. 57*, 1267–1270.

Srajer, V., Reinisch, L., & Champion, P. (1988) *J. Am. Chem. Soc. 110*, 6656–6661.

Valat, P., & Alpert, B. (1985) *Laser Chem. 5*, 173–183.